

MATHEMATICAL MODELING OF PATTERN FORMATION IN SUB- AND SUPERDIFFUSIVE REACTION-DIFFUSION SYSTEMS

VASYL GAFIYCHUK*, BOHDAN DATSKO†, AND VITALIY MELESHKO‡

Abstract. This paper is concerned with analysis of coupled fractional reaction-diffusion equations. It provides analytical comparison for the fractional and regular reaction-diffusion systems. As an example, the reaction-diffusion model with cubic nonlinearity and Brusselator model are considered. The detailed linear stability analysis of the system with cubic nonlinearity is provided. It is shown that by combining the fractional derivatives index with the ratio of characteristic times, it is possible to find the marginal value of the index where the oscillatory instability arises. Computer simulation and analytical methods are used to analyze possible solutions for a linearized system. A computer simulation of the corresponding nonlinear fractional ordinary differential equations is presented. It is shown that the increase of the fractional derivative index leads to the periodic solutions which become stochastic at the index approaching the value of 2. It is established by computer simulation that there exists a set of stable spatio-temporal structures of the one-dimensional system under the Neumann and periodic boundary condition. The characteristic features of these solutions consist in the transformation of the steady state dissipative structures to homogeneous oscillations or space temporary structures at a certain value of fractional index.

Key words. reaction-diffusion system, fractional differential equations, oscillations, dissipative structures, pattern formation, spatio-temporal structures

AMS subject classifications. 37N30, 65P40, 37N25, 35K50, 35K45, 34A34, 34C28, 65P30

1. Introduction. Reaction-diffusion (RD) systems are inherent in many branches of physics, chemistry, biology, ecology etc. The review of the theory and applications of reaction-diffusion systems one can find in books and numerous articles (See, for example [1, 2, 3, 4, 5, 6, 7, 8, 9, 10, 11]). The popularity of the RD system is driven by the underlying richness of the nonlinear phenomena, which include stationary and spatio-temporary dissipative pattern formation, oscillations, different types of chemical waves, excitability, bistability etc. The mechanism of the formation of such type of nonlinear phenomena and the conditions of their emergence have been extensively studied during the last couple decades. Although the mathematical theory of such type of phenomena has not been developed yet due to the essential nonlinearity of these systems, from the viewpoint of the applied and experimental mathematics, the pattern of possible phenomena in RD system is more or less understandable.

In the recent years, there has been a great deal of interest in fractional reaction-diffusion (FRD) systems [12, 13, 14, 15, 16, 17, 18, 19, 20, 21] which from one side exhibit self-organization phenomena and from the other side introduce a new parameter to these systems, which is a fractional derivative index, and it gives a greater degree of freedom for diversity of self-organization phenomena. At the same time, the process of analyzing such FRD systems is much complicated from the analytical and numerical point of view.

In this article, we consider two coupled reaction-diffusion systems:

The first one is the classical system

*Institute of Applied Problem of Mechanics and Mathematics, National Academy of Sciences of Ukraine, Naukova Street 3 B, Lviv, Ukraine 79053(viva@iapmm.lviv.ua)

†Institute of Applied Problem of Mechanics and Mathematics, National Academy of Sciences of Ukraine, Naukova Street 3 B, Lviv, Ukraine 79053(viva@iapmm.lviv.ua)

‡Institute of Applied Problem of Mechanics and Mathematics, National Academy of Sciences of Ukraine, Naukova Street 3 B, Lviv, Ukraine 79053(viva@iapmm.lviv.ua)

$$(1.1) \quad \tau_1 \frac{\partial n_1(x, t)}{\partial t} = l^2 \nabla^2 n_1(x, t) - W(n_1, n_2, \mathcal{A}),$$

$$(1.2) \quad \tau_2 \frac{\partial n_2(x, t)}{\partial t} = L^2 \nabla^2 n_2(x, t) - Q(n_1, n_2, \mathcal{A}),$$

where $x, t \in \mathbb{R}$; $\nabla^2 = \frac{\partial^2}{\partial x^2}$; $n_1(x, t), n_2(x, t) \in \mathbb{R}$ – two variables, $W, Q \in \mathbb{R}$ are the nonlinear sources of the system modeling their production rates, $\tau_1, \tau_2, l, L, \in \mathbb{R}$ – characteristic times and lengths of the system, $\mathcal{A} \in \mathbb{R}$ – is an external parameter

And the other model is the fractional RD system

$$(1.3) \quad \tau_1 \frac{\partial^\alpha n_1(x, t)}{\partial t^\alpha} = l^2 \nabla^2 n_1(x, t) - W(n_1, n_2, \mathcal{A}),$$

$$(1.4) \quad \tau_2 \frac{\partial^\alpha n_2(x, t)}{\partial t^\alpha} = L^2 \nabla^2 n_2(x, t) - Q(n_1, n_2, \mathcal{A})$$

with the same parameters and fractional derivatives $\frac{\partial^\alpha n(x, t)}{\partial t^\alpha}$ on the left hand side of equations (1.3),(1.4) instead of standard time derivatives, which are the Caputo fractional derivatives in time of the order $0 < \alpha < 2$ and are represented as [23, 24]

$$\frac{\partial^\alpha n(t)}{\partial t^\alpha} := \frac{1}{\Gamma(m - \alpha)} \int_0^t \frac{n^{(m)}(\tau)}{(t - \tau)^{\alpha + 1 - m}} d\tau, \quad m - 1 < \alpha < m, m \in \mathbb{N}.$$

The article is devoted to the second problem and the first one we need for comparing the obtained results with classical one.

Equations (1.3),(1.4) at $\alpha = 1$ correspond to standard RD system described by equations (1.1),(1.2). At $\alpha < 1$, they describe anomalous sub-diffusion and at $\alpha > 1$ - anomalous superdiffusion .

In this paper, we always assume that the following conditions are fulfilled on the boundaries $0; l_x$:

(i) Neumann:

$$(1.5) \quad dn_i/dx|_{x=0} = dn_i/dx|_{x=l_x} = 0$$

(ii) Periodic:

$$(1.6) \quad n_i(t, 0) = n_i(t, l_x), \quad dn_i/dx|_{x=0} = dn_i/dx|_{x=l_x},$$

where $i = 1, 2$.

2. Linear stability analysis. Stability of the steady-state constant solutions of the system (1.3),(1.4) correspond to homogeneous equilibrium states

$$(2.1) \quad W(n_1, n_2, \mathcal{A}) = 0, \quad Q(n_1, n_2, \mathcal{A}) = 0$$

can be analyzed by linearization of the system nearby this solution. In this case the system (1.3)(1.4) can be transformed to linear system

$$(2.2) \quad \frac{\partial^\alpha \mathbf{u}(x, t)}{\partial t^\alpha} = \hat{A} \mathbf{u}(x, t),$$

where $\mathbf{u}(x, t) = \begin{pmatrix} \Delta n_1(x, t) \\ \Delta n_2(x, t) \end{pmatrix}$, $\hat{A} = \begin{pmatrix} (l^2 \nabla^2 - a_{11})/\tau_1 & -a_{12}/\tau_1 \\ -a_{21}/\tau_2 & (L^2 \nabla^2 - a_{22})\tau_2 \end{pmatrix}$, $a_{11} = W'_{n_1}$, $a_{12} = W'_{n_2}$, $a_{21} = Q'_{n_1}$, $a_{22} = Q'_{n_2}$ (all derivatives are taken at homogeneous equilibrium states (condition (2.1))). By substituting the solution $\mathbf{u}(x, t) = \begin{pmatrix} \Delta n_1(t) \\ \Delta n_2(t) \end{pmatrix} \cos kx$, $k = \frac{\pi}{L}j$, $j = 1, 2, \dots$ into FRD system (1.3),(1.4) we can get the system of linear ordinary differential equations (2.2) with the matrix A determined by the operator \hat{A} , the stability conditions of which are given by eigenvalues of this matrix.

Let us analyze the stability of the solution (2.1) of the linear system with integer derivatives and find the conditions of this instability (See, for example:[2, 3, 4, 5]). We repeat this process in order to compare the results obtained with the results of the fractional RD system considered in this article. In this case, by searching for the solution of the linear system in the form $\mathbf{u}(x, t) = \begin{pmatrix} \Delta n_1 \\ \Delta n_2 \end{pmatrix} \exp(\lambda t) \cos kx$, we get a homogeneous system of linear algebraic equations for constants $\Delta n_1, \Delta n_2$. The solubility of this system leads to the characteristic equation

$$(2.3) \quad \det |\lambda I - A| = 0,$$

where

$$(2.4) \quad A = - \begin{pmatrix} (l^2 k^2 + a_{11})/\tau_1 & a_{12}/\tau_1 \\ a_{21}/\tau_2 & (L^2 k^2 + a_{22})/\tau_2 \end{pmatrix},$$

I is the identity matrix. As a result, the characteristic equation takes on a form of a simple quadratic equation $\lambda^2 - \text{tr} A \lambda + \det A = 0$.

The linear boundary value problem for RD system (1.1),(1.2) is unstable according to inhomogeneous wave vectors $k \neq 0$ if ($\text{tr} A < 0, \det A < 0$)

$$(2.5) \quad a_{11} < -[(l/L)^2 a_{22} + 2(l/L)(a_{22} a_{11} - a_{12} a_{21})^{1/2}],$$

$$\tau_2(a_{11} + k^2 l^2) + \tau_1(a_{22} + k^2 L^2) > 0, \quad a_{22} a_{11} - a_{12} a_{21} > 0$$

(Turing Bifurcation) and according to homogenous ($k = 0$) fluctuations (Hopf Bifurcation) if ($\text{tr} A > 0, \det A > 0$)

$$(2.6) \quad \tau_2 a_{11} + \tau_1 a_{22} < 0, \quad a_{22} a_{11} - a_{12} a_{21} > 0.$$

For analyzing the equations (1.3),(1.4) let us also consider a linear system obtained near the homogeneous state (2.1). As a result, the simple linear transformation can convert this linear system to a diagonal form

$$(2.7) \quad \frac{d^\alpha \eta(t)}{dt^\alpha} = C \eta(t),$$

where C is a diagonal matrix of A : $C = P^{-1} A P = \begin{pmatrix} \lambda_1 & 0 \\ 0 & \lambda_2 \end{pmatrix}$, eigenvalues $\lambda_{1,2}$ are determined by the same characteristic equation (2.3) with matrix (2.4), $\lambda_{1,2} =$

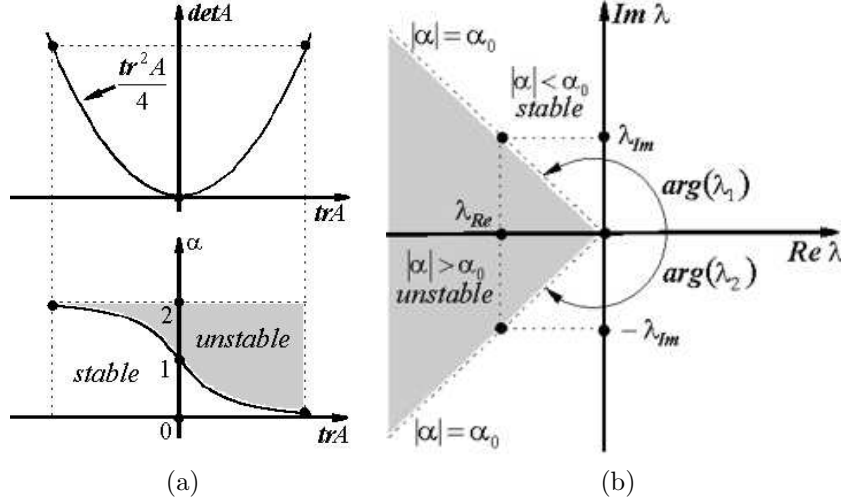


FIG. 2.1. Schematic view of the marginal curve describing fixed points for two-dimensional vector field – (a) the marginal value of α – (b).

$\frac{1}{2}(trA \pm \sqrt{tr^2A - 4 \det A})$, $\eta(t) = P^{-1} \begin{pmatrix} \Delta n_1(t) \\ \Delta n_2(t) \end{pmatrix}$, P is the matrix of eigenvectors of matrix A .

In this case, the solution of the vector equation (2.7) is given by Mittag-Leffler functions [23, 24, 25, 26, 22]

$$(2.8) \quad \Delta n_i(t) = \sum_{k=0}^{\infty} \frac{(\lambda_i t^\alpha)^k}{\Gamma(k\alpha + 1)} \Delta n_i(0) = E_\alpha(\lambda_i t^\alpha) \Delta n_i(0), \quad i = 1, 2.$$

Using the result obtained in the papers [18, 32], we can conclude that if for any of the roots

$$(2.9) \quad |\arg(\lambda_i)| < \alpha\pi/2$$

the solution has an increasing function component then the system is asymptotically unstable.

Analyzing the roots of the characteristic equations, we can see that at $4 \det A - tr^2A > 0$ eigenvalues are complex and can be represented as

$$\lambda_{1,2} = \frac{1}{2}(trA \pm i\sqrt{4 \det A - tr^2A}) \equiv \lambda_{Re} \pm i\lambda_{Im}.$$

The roots $\lambda_{1,2}$ are complex inside the parabola (Figure 2.1(a)) and the fixed points are the spiral source ($trA > 0$) or spiral sinks ($trA < 0$). The plot of the marginal value $\alpha : \alpha = \alpha_0 = \frac{2}{\pi}|\arg(\lambda_i)|$ which follows from the conditions (2.9) is given by the formula

$$(2.10) \quad \alpha_0 = \begin{cases} \frac{2}{\pi} \arctan \sqrt{4 \det A / tr^2A - 1}, & trA \geq 0, \\ 2 - \frac{2}{\pi} \arctan \sqrt{4 \det A / tr^2A - 1}, & trA \leq 0 \end{cases}$$

and is presented in the Figure 2.1(a) below the parabola in the coordinate system (trA, α) .

Let us analyze the system solution with the help of the Figure 2.1(a). Consider the parameters which keep the system inside the parabola. It is a well-known fact, that at $\alpha = 1$ the domain on the righthand side of the parabola ($trA > 0$) is unstable with the existing limit circle, while the domain on the left hand side ($trA < 0$) is stable. By crossing the axis $trA = 0$ the Hopf bifurcation conditions become true. In the general case of $\alpha : 0 < \alpha < 2$ for every point inside the parabola there exists a marginal value of α_0 where the system changes its stability. The value of α is a certain bifurcation parameter which switches the stable and unstable state of the system. At lower $\alpha : \alpha < \alpha_0 = \frac{2}{\pi}|\arg(\lambda_i)|$ the system has oscillatory modes but they are stable. Increasing the value of $\alpha > \alpha_0 = \frac{2}{\pi}|\arg(\lambda_i)|$ leads to instability. As a result, the domain below the curve α_0 , as a function of trA is stable and the domain above the curve is unstable.

The plot of the roots, describing the mechanism of the system instability, can be understood from the Figure 2.1(b) where the case $\alpha_0 > 1$ is described. In fact, having complex number λ_i with $Re\lambda_i < 0$ at $\alpha \rightarrow 2$ it is always possible to satisfy the condition $|\arg(\lambda_i)| < \alpha\pi/2$, and the system becomes unstable according to homogeneous oscillations (Figure 2.1(b)). The smaller is the value of trA , the easier it is to fulfill the instability conditions.

In contrast to this case, a complex values of λ_i , with $Re\lambda_i > 0$ lead to the system instability for regular system with $\alpha = 1$. However fractional derivatives with $\alpha < 1$ will stabilize the system if $\alpha < \alpha_0 = \frac{2}{\pi}|\arg(\lambda_i)|$. This makes it possible to conclude that fractional derivative equations with $\alpha < 1$ are more stable than their integer twinges.

3. Solutions of the coupled fractional ordinary differential equations (FODEs). Our particular interest here is the analysis of the specific non-linear system of FRD equations. We consider two very well-known examples. The first one is the RD system with cubical nonlinearity [3, 4, 7] which probably is the simplest one used in RD systems modeling

$$(3.1) \quad W(n_1, n_2) = -n_1 + n_1^3/3 + n_2, \quad Q = n_2 - \beta n_1 - \mathcal{A}.$$

The second example is known as Brusselator model [1] and it describes certain chemical reaction-diffusion processes with a pair of variables whose concentrations are controlled by nonlinearities

$$(3.2) \quad W(n_1, n_2) = -\mathcal{A} + (\beta + 1)n_1 - n_1^2 n_2, \quad Q(n_1, n_2) = -\beta n_1 + n_1^2 n_2,$$

Let us first consider the coupled fractional ordinary differential equations (FODEs) with nonlinearities (3.1) and analyze the stability conditions for such systems. The plot of isoclines for the system (3.1) is represented on Figure 3.1(a). In this case, for homogeneous solution, which can be determined from the system of equations $W = Q = 0$, is the solution of cubic algebraic equation $(\beta - 1)\bar{n}_1 + \bar{n}_1^3/3 + \mathcal{A} = 0$. Simple calculation makes it possible to write the expressions required for analysis $A = -\begin{pmatrix} (-1 + \bar{n}_1^2)/\tau_1 & 1/\tau_1 \\ -\beta/\tau_2 & 1/\tau_2 \end{pmatrix}$, $trA = (1 - \bar{n}_1^2)/\tau_1 - 1/\tau_2$, $\det A = ((\beta - 1) + \bar{n}_1^2)/\tau_1 \tau_2$.

It is easy to see that if the value of τ_1/τ_2 , in certain cases, is smaller than 1, the instability conditions ($trA > 0$) lead to Hopf bifurcation for regular system ($\alpha = 1$) [1, 2, 3, 4, 5]. In this case, the plot of the domain, where instability exists, is shown on the Figure 3.1(b).

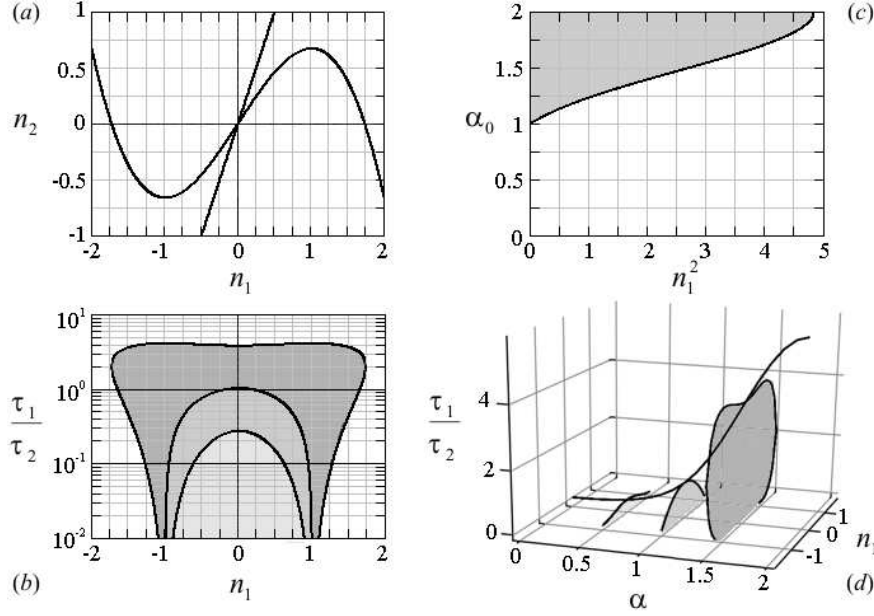


FIG. 3.1. Null isoclines – (a), Instability domains (shaded regions) in coordinates $(\bar{n}_1, \tau_1/\tau_2)$ (Dependence of τ_1/τ_2 on \bar{n}_1) – (b), Dependence of α_0 on \bar{n}_1^2 – (c), Dependence of τ_1/τ_2 on α_0 (the domains in coordinates $(\bar{n}_1, \tau_1/\tau_2)$ correspond to domains represented on figure (b) – (d)).

The linear analysis of the system for $\alpha = 1$ shows that, if $\tau_1/\tau_2 > 1$, the solution corresponds to the intersections of two isoclines, and it is stable. The marginal curve, separating stability and instability domains, is given on Figure 3.1(b). The smaller is the ratio of τ_1/τ_2 , the wider is the instability region. Formally, at $\tau_1/\tau_2 \rightarrow 0$, the instability region in \bar{n}_1 coincides with the interval $(-1, 1)$ where the null isocline $W(n_1, n_2) = 0$ has its increasing part. The maximum value of the curve $\tau_1/\tau_2(n_1)$ corresponds to the value $\tau_1/\tau_2 = 1$ where the system is neutrally stable. These results are very widely known in the theory of nonlinear dynamical systems [1, 2, 3, 4, 5].

In the FODEs the conditions of the instability change (2.9), and we have to analyze the real and the imaginary part of the existing complex eigenvalues, especially the equation: $4 \det A - tr^2 A = 4((\beta - 1) + \bar{n}_1^2)/\tau_1\tau_2 - ((1 - \bar{n}_1^2)/\tau_1 - 1/\tau_2)^2 > 0$. In fact, with the complex eigenvalues, it is possible to find out the corresponding value of α where the condition (2.9) is true. We show that this interval is not correlated with the increasing part of the null isocline of the system. Indeed, omitting simple calculation, we can write an equation for marginal values of \bar{n}_1 : $\bar{n}_1^4 - 2(1 + \frac{\tau_1}{\tau_2})\bar{n}_1^2 + \frac{\tau_1^2}{\tau_2^2} - 2\frac{\tau_1}{\tau_2}(2\beta - 1) + 1 = 0$, and expression $\bar{n}_1^2 = 1 + \frac{\tau_1}{\tau_2} \pm 2\sqrt{\beta\frac{\tau_1}{\tau_2}}$ estimates the maximum and minimum values of \bar{n}_1 where the system can be unstable at certain value of $\alpha = \alpha_0$. For example, examine the domain of the FODEs where the eigenvalues are complex for fixed value τ_1/τ_2 , for example, consider $\tau_1 = \tau_2 = 1$ and $\beta = 2$. In this case, $trA = -\bar{n}_1^2$, $\det A = 1 + \bar{n}_1^2$, $4 \det A - tr^2 A = 4 + 4\bar{n}_1^2 - \bar{n}_1^4 > 0$, which immediately leads to the region of existing of complex roots $-\sqrt{2 + 2\sqrt{2}} \leq \bar{n}_1 \leq \sqrt{2 + 2\sqrt{2}}$ and we can conclude that the instability region, due to the fractional order of the derivatives, can be much wider than the same region for $(\alpha = 1)$. The dependance of the value of

α on the value \bar{n}_1^2 (2.10) is given on Figure 3.1(c).

In this case the plot is obtained at $\tau_1/\tau_2 = 1$ and that is why the marginal instability curve is determined for $\alpha > 1$ (for $\alpha < 1$ the system is stable). On this figure the domain below the curve corresponds to stability and above it to instability conditions.

Similar analysis can be provided for $trA > 0$ where (τ_1/τ_2) is smaller than unity. In this case, the instability conditions are also not correlated with the increasing part of the null isocline $W_1(n_1, n_2)$. In this case the plot of α will be start not from 1 but from certain value smaller than unity. However, it is much better for understanding to get marginal curve α_0 as a function of τ_1/τ_2 .

Let us analyze the dependence of α_0 on the parameter τ_1/τ_2 where the system changes its stability. As it is easy to see from Figure 3.1(a),(b) that the easiest way to reach instability domain is realized at $\mathcal{A} = 0$ when two isoclines are intersected themselves at the point $(0, 0)$ and this corresponds to maximum of the curve on Figure 3.1(b). Let us consider the dependence of this marginal value of α_0 on the parameter τ_1/τ_2 at $\mathcal{A} = 0$ and determine the plot of this maximum as a functions of α_0 on τ_1/τ_2 . Such curve for the given model is represented in the Figure 3.1(d). This curve obtained from (2.10) corresponds to the dependence of α on trA (Figure 2.1(a)). Below this curve the system is unstable, and above it - it is stable. We may therefore focus our attention on the general form of this curve. At sufficiently small value τ_1/τ_2 oscillatory instability is valid even for small $\alpha < 1$. In contrast, at $\alpha > 1$, the instability conditions could have place even for those cases when τ_1/τ_2 is sufficiently large. This means that fractional differential equations, by corresponding combination of the parameter τ_1/τ_2 , can be stable or unstable practically in all the region $1 < \alpha < 2$.

It should be noted that, even if the eigenvalues are not complex ($\lambda_{Im} = 0$), the systems with fractional derivatives can poses oscillatory damping oscillations. Such situation takes place when $4 \det A - tr^2 A < 0$, $trA < 0$, $\det A > 0$ and two eigenvalues are real and less than zero. In this case, at $1 < \alpha < 2$ steady state solutions of the system are stable and any perturbations are damping. Such system was considered, for example, in the article [31], where an analytical solution for fractional oscillator is obtained. Namely with this case we start analyzing possible solutions.

Several examples of linear FDOEs were solved analytically by Adomian decomposition method, as well as numerically. The obtained solutions were compared with the analytical solutions obtained by Mittag-Leffler functions (2.8) and the results of the work [31].

Three different solutions are plotted on the same Figure 3.2. The results of the computer simulation of linear ordinary differential equations for stable system - a) and unstable system - b) of one variable n_1 are given on the time domain interval $[0, 30]$. We can see that in the stable domain $\alpha < \alpha_0$ the oscillations are damping, and at $\alpha > \alpha_0$ they grow exponentially. So, the ordinary differential equations (space derivatives are equal to zero) of the system have two different modes. The solution is either asymptotically stable or unstable.

It is a statement, that FODEs are at least as stable as their integer order counterparts [24]. At the same time, we have established here that the dynamics of the FODEs can be much more complicated than that of the equations with integer order [33, 32, 34]. Our task here is to clarify these statements by finding out not only the conditions of the bifurcation but also the real time dynamics of FODEs.

The developed technique of Adomian decomposition [27, 28, 29, 30] is a powerful

method for solving the system of ordinary differential equations. The effectiveness of this method was demonstrated for solving linear fractional differential equations, and we used this method here to test the computer program and to compare these analytical results with Mittag-Leffler functions.

First, we consider the case when the system is always asymptotically stable at $\alpha < \alpha_0 = 2$, for example $\alpha = 1.7$ (Figure 3.2(a)). Three solutions obtained by these different methods practically do not differ from each other and they show oscillatory damping time behavior (the model described in [31]). Analytical results obtained by Adomian decomposition is given by the formula

$$(3.3) \quad n_1 = \sum_{k=0}^{\infty} (-1)^k \frac{t^{k\alpha}}{\Gamma(k\alpha + 1)},$$

which is plot on the Figure 3.2(a) by empty circled curve (we truncate the series at $k=60$). At small time interval (for example $t < 7$) this series can be represented by next expansion

$$\begin{aligned} n_1 = & 1 - 0.6473808267 \cdot t^{1.7} + 0.9865725648 \cdot 10^{-1} \cdot t^{3.4} - 0.7019911214 \cdot 10^{-2} \cdot t^{5.1} \\ & + 0.296127716 \cdot 10^{-3} \cdot t^{6.8} - 0.838275933 \cdot 10^{-5} \cdot t^{8.5} + 0.171848173 \cdot 10^{-6} \cdot t^{10.2} \\ & - 0.2686528893 \cdot 10^{-8} \cdot t^{11.9} + 0.3324725330 \cdot 10^{-10} \cdot t^{13.6} \\ & - 0.3350625811 \cdot 10^{-12} \cdot t^{15.3} + 0.2811457252 \cdot 10^{-14} \cdot t^{17}. \end{aligned}$$

Despite the considered system, in this particular case, cannot be unstable (Figure 3.2(a)) because the values of λ are real and negative $|\arg(\lambda_1)| = \pi > \alpha\pi/2$, in the limit at $\alpha = 2$ we have a regular linear oscillator [31], analytical solution of which we get from Adomian decomposition in the form of power series. The terms of this series completely coincides with the expansion of linear oscillator solution $\cos(x)$.

It should be noted that all damped oscillations solutions of the linear oscillator of fractional order have similar plots.

Quite different is the dynamics of FODEs for $\alpha > \alpha_0$ when oscillatory mode becomes unstable and leads to increasing oscillations at $\alpha > \alpha_0$ (Figure 3.2(b)). In this case, the analytical solution obtained by Adomian decomposition for $\alpha = 1.3$ looks like

$$\begin{aligned} n_1 = & 0.67 - 0.1716397314 \cdot t^{1.3} - 0.05663459553 \cdot t^{2.6} + 0.008906834532 \cdot t^{3.9} \\ & + 0.00006991997714 \cdot t^{5.2} - 0.00004692163249 \cdot t^{6.5} + 0.1292316598 \cdot 10^{-5} \cdot t^{7.8} \\ & + 0.5298004324 \cdot 10^{-7} \cdot t^{9.1} - 0.2781417477 \cdot 10^{-8} \cdot t^{10.4} \\ & + 0.3895105489 \cdot 10^{-11} \cdot t^{11.7} + 0.1811701048 \cdot 10^{-11} \cdot t^{13} + \dots \end{aligned}$$

The result of taking into account 50 terms in Adomian decomposition expansion makes it possible to represent the solution in the time interval till $t = 30$ is presented on the Figure 3.2(b). As a matter of fact, such representation has rather theoretical sense because our system is essentially nonlinear and does not allow this type of solutions. For the initial stage dynamics or for the linear system, Adomian decomposition method is very effective. The application of Adomian decomposition to the nonlinear FDOEs is not successful. Taking into account 10 terms makes it possible to find out the solution on time interval $t = 6 - 7$ and at higher values of t the discrepancy between the numerical solution and the one, obtained by Adomian decomposition, increases rapidly.

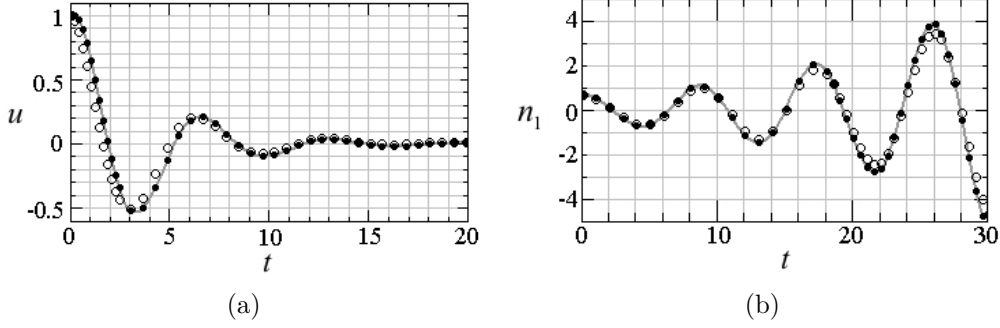


FIG. 3.2. The damped oscillator solution for $\frac{\partial^\alpha u}{\partial t^\alpha} = -u$ at $\alpha = 1.7$, $u(0) = 1 - (a)$, and the increasing time domain oscillations of the linearized system (1.3),(1.4) for n_1 and $\alpha = 1.3$, $\mathcal{A} = -0.1$, $\beta = 1$, $\tau_1 = \tau_2 = 1$, $n_1(0) = (-3\mathcal{A})^{\frac{1}{3}}$, $n_2(0) = (-3\mathcal{A})^{\frac{1}{3}} + \mathcal{A} - (b)$. Small filled circled line - Mittag-Leffler solution, empty circled line - Adomian decomposition solution, solid gray line - numerical solution

To demonstrate the nontrivial properties of FDOEs, here we consider the nonlinear dynamics of the above mentioned nonlinear fractional differential equations.

For $\alpha > \alpha_0$ small perturbation of the steady state solution, due to the memory inherent in fractional derivatives survive in the process of evolution and grow in amplitude while nonlinear terms of the system (3.1) restrict the value of these oscillations. In this case, time dependence of the variables corresponds to the oscillatory solution. (The phase portrait and isoclines are presented on Figure 3.3(a)-(e)).

Analyzing the phase trajectory of the FODEs, we can see that the amplitude of the oscillations increases with increasing α . At α approaching 2, the oscillations become more complicated and at $\alpha = 2$ they look more quasichaotic. The time dependence of this solution is represented in Figure 3.3(f).

Brusselator system with nonlinearities (3.2) has quite similar behavior. Calculating, for example, at $\mathcal{A} = 2$, $\beta = 2$, $\tau_1 = \tau_2 = 1$ the value of α_0 we find that $\alpha_0 = 1.54$.

The phase portrait and isoclines for (3.2) are presented in Figure 3.4 (a)-(c). At $\alpha \lesssim 1.5$, we obtain steady state solution and at $\alpha \gtrsim 1.5$ - the steady state oscillation. The increase of the value α leads to the complication of the phase paths, and the two-dimensional phase portrait looks much more complicated (Figure 3.4(b)-(c)). The attractor of the system of the two coupled nonlinear differential equations gets the features of strange attractor and at $\alpha \rightarrow 2$ it corresponds to the attractor of the fourth order differential equations determined by the nonlinearities (3.2).

4. Computer simulation of pattern formation. This section contains a discussion of the results of the numerical study of the initial value problem of the system (1.3)(1.4). The system with corresponding initial and boundary conditions was integrated numerically using the explicit and implicit schemes with respect to time and centered difference approximation for spatial derivatives. The fractional derivatives were approximated using two different schemes on the basis Riemann-Liouville definition : $L1$ -scheme for $0 \leq \alpha < 1$, $L2$ -scheme for $1 \leq \alpha < 2$ (see below and [35]), as well as the scheme on the basis of Grunwald-Letnikov definition for $0 < \alpha < 1$ and $1 < \alpha < 2$ [24] . In other words, for the system of n fractional RD equations

$$(4.1) \quad \tau_j \frac{{}^C \partial^{\alpha_j} u_j(x, t)}{\partial t^{\alpha_j}} = d_j \frac{\partial^2 u_j(x, t)}{\partial x^2} + f_j(u_1, \dots, u_n), \quad j = \overline{1, n},$$

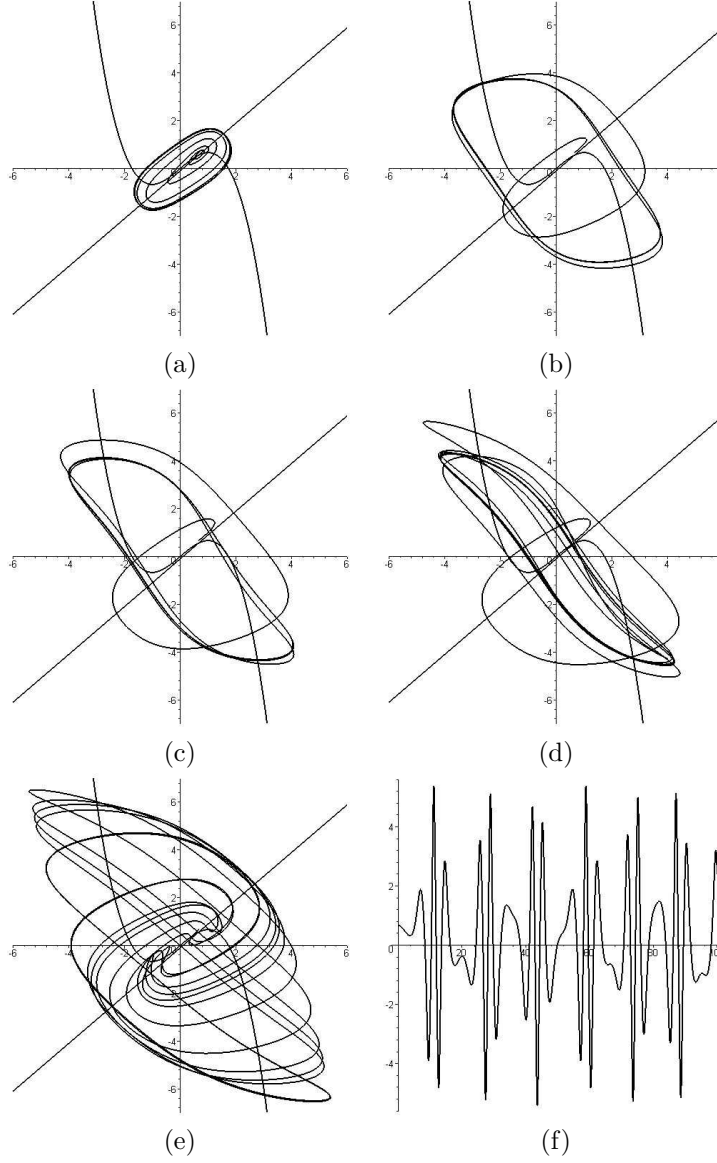


FIG. 3.3. Two dimensional phase portrait (a)-(e) and time domain oscillations corresponding to plot (e) - (f) of the system (1.3), (1.4) with nonlinearities (3.1) for $\mathcal{A} = -0.1, \beta = 1, \tau_1 = \tau_2 = 1, l = L = 0$. (a) - $\alpha=1.3$, (b) - $\alpha=1.7$, (c) - $\alpha=1.8$, (d) - $\alpha=1.90$, (e) - $\alpha=2.0$, time domain oscillations (f) - $\alpha=2.00$

where τ_j, d_j, f_j - certain parameters and nonlinearities of the RD system correspondingly, we used the next numerical schemes:

L1-scheme

$$\delta_j u_{j,i}^k - \frac{d_j}{(\Delta x)^2} (u_{j,i-1}^k - 2u_{j,i}^k + u_{j,i+1}^k) - f_j(u_{1,i}^k, \dots, u_{n,i}^k) =$$

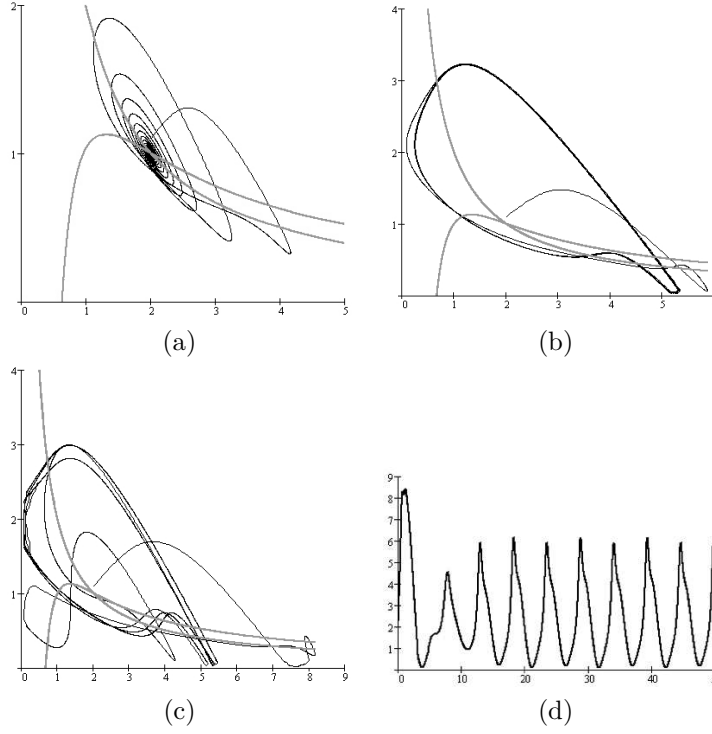


FIG. 3.4. Two dimensional phase portrait (a)-(c) and time domain oscillations corresponding to plot (c) - (d) of the system (1.3), (1.4) with nonlinearities (3.2) for $A = 2, \beta = 2, \tau_1 = \tau_2 = 1, l = L = 0$. (a) - $\alpha=1.5$, (b) - $\alpha=1.6$, (c) - $\alpha=1.7$, time domain oscillations (d) - $\alpha=1.7$

$$= -\delta_j \left(u_{j,i}^0 w_k^{(\alpha_j)} + \sum_{l=1}^{k-1} u_{j,i}^l \beta_{k-l+1}^{(\alpha_j)} \right) + \tau_j \frac{(k\Delta t)^{-\alpha_j}}{\Gamma(1-\alpha_j)} u_{j,i}^0$$

$$\delta_j = \frac{\tau_j (\Delta t)^{-\alpha_j}}{\Gamma(2-\alpha_j)}, \quad w_k^{(\alpha_j)} = \frac{1-\alpha_j}{k^{\alpha_j}} - k^{1-\alpha_j} - (k-1)^{1-\alpha_j},$$

$$\beta_s^{(\alpha_j)} = s^{1-\alpha_j} - 2(s-1)^{1-\alpha_j} + (s-2)^{1-\alpha_j}, \quad s = \overline{2, k};$$

L2-scheme

$$\begin{aligned} & \delta_j u_{j,i}^{k+1} - \frac{d_j}{\Delta x^2} (u_{j,i-1}^{k+1} - 2u_{j,i}^{k+1} + u_{j,i+1}^{k+1}) - f_j(u_{1,i}^{k+1}, \dots, u_{n,i}^{k+1}) = \\ & = -\delta_j [u_{j,i}^0 w_{0,k}^{\alpha_j} + u_{j,i}^1 w_{1,k}^{\alpha_j} + \sum_{l=2}^{k-1} u_{j,i}^l \beta_{k-l+2}^{(\alpha_j)} + u_{j,i}^k (2^{2-\alpha_j} - 3)] + \tau_j \sum_{p=0}^m \frac{(k\Delta t)^{p-\alpha_j}}{\Gamma(p-\alpha_j+1)} \frac{\partial^p}{\partial t^p} u_{j,i}^0, \end{aligned}$$

$$\delta_j = \frac{\tau_j (\Delta t)^{-\alpha_j}}{\Gamma(3-\alpha_j)}, \quad w_{0,k}^{\alpha_j} = \frac{(1-\alpha_j)(2-\alpha_j)}{k^{\alpha_j}} - \frac{(2-\alpha_j)}{k^{\alpha_j-1}} + k^{2-\alpha_j} - (k-1)^{2-\alpha_j},$$

$$w_{1,k}^{\alpha_j} = \frac{(2 - \alpha_j)}{k^{\alpha_j - 1}} - 2k^{2 - \alpha_j} + 3(k - 1)^{2 - \alpha_j} - (k - 2)^{2 - \alpha_j},$$

$$\beta_s^{(\alpha_j)} = s^{2 - \alpha_j} - 3(s - 1)^{2 - \alpha_j} + 3(s - 2)^{2 - \alpha_j} - (s - 3)^{2 - \alpha_j}, \quad s = \overline{3, k}$$

and **G-L scheme**

$$u_{j,i}^k - \frac{d_j(\Delta t)^{\alpha_j}}{\tau_j(\Delta x)^2} (u_{j,i-1}^k - 2u_{j,i}^k + u_{j,i+1}^k) - \frac{(\Delta t)^{\alpha_j}}{\tau_j} f_j(u_{1,i}^k, \dots, u_{n,i}^k) =$$

$$= (\Delta t)^{\alpha_j} \sum_{p=0}^m \frac{(k\Delta t)^{p - \alpha_j}}{\Gamma(p - \alpha_j + 1)} \frac{\partial^p}{\partial t^p} u_{j,i}^0 - \sum_{l=1}^k c_l^{(\alpha_j)} u_{j,i}^{k-l},$$

$$c_0^{(\alpha_j)} = 1, \quad c_l^{(\alpha_j)} = c_{l-1}^{(\alpha_j)} \left(1 - \frac{1 + \alpha_j}{l} \right), \quad l = 1, 2, \dots$$

where $u_{j,i}^k \equiv u_j(x_i, t_k) \equiv u_j(i\Delta x, k\Delta t)$, $m = [\alpha]$.

The applied numerical schemes are implicit, and for each time layer they are presented as the system of algebraic equations solved by Newton-Raphson technique. Such approach makes it possible to get the system of equations with band Jacobian for each node and to use the sweep method for the solution of linear algebraic equations. Calculating the values of the spatial derivatives and corresponding nonlinear terms on the previous layer, we obtained explicit schemes for integration. Despite the fact that these algorithms are quite simple, they are very sensitive and require small steps of integration, and they often do not allow to find numerical results. In contrast, the implicit schemes, in certain sense, are similar to the implicit Euler's method, and they have shown very good behavior at the modeling of fractional reaction-diffusion systems for different step size of integration, as well as for nonlinear function and the power function of fractional index. Moreover, by modeling according to this algorithm system (1.1),(1.2), we have observed that these results fully match the results obtained prior.

It should be noted that the definition of the fractional derivative in Grunwald-Letnikov form is equivalent to the one in Riemann-Liouville method, but for numerical calculations it is much more flexible.

We have considered here the kinetics of formation of dissipative structures for different values of α . These results are presented on Figures 4.1 and 4.2.

The simulations were carried out for a one-dimensional system on an equidistant grid with spatial step h changing from $= 0.1$ to 0.01 and time step Δt changing from 0.001 to 0.1 . We used imposed Neuman (1.5) or periodic boundary conditions (1.6). As the initial condition, we used the uniform state which was superposed with a small spatially inhomogeneous perturbation.

The systems have rich dynamics, including steady state dissipative structures, homogeneous and nonhomogeneous oscillations, and spatiotemporal patterns. In this paper, we focus mainly on the study of general properties of the solutions depending on the value of α .

As discussed in Section 2, there are two different regions in parameter \mathcal{A} , where the system can be stable or unstable. In the case of $\alpha = 1$ the steady state solutions

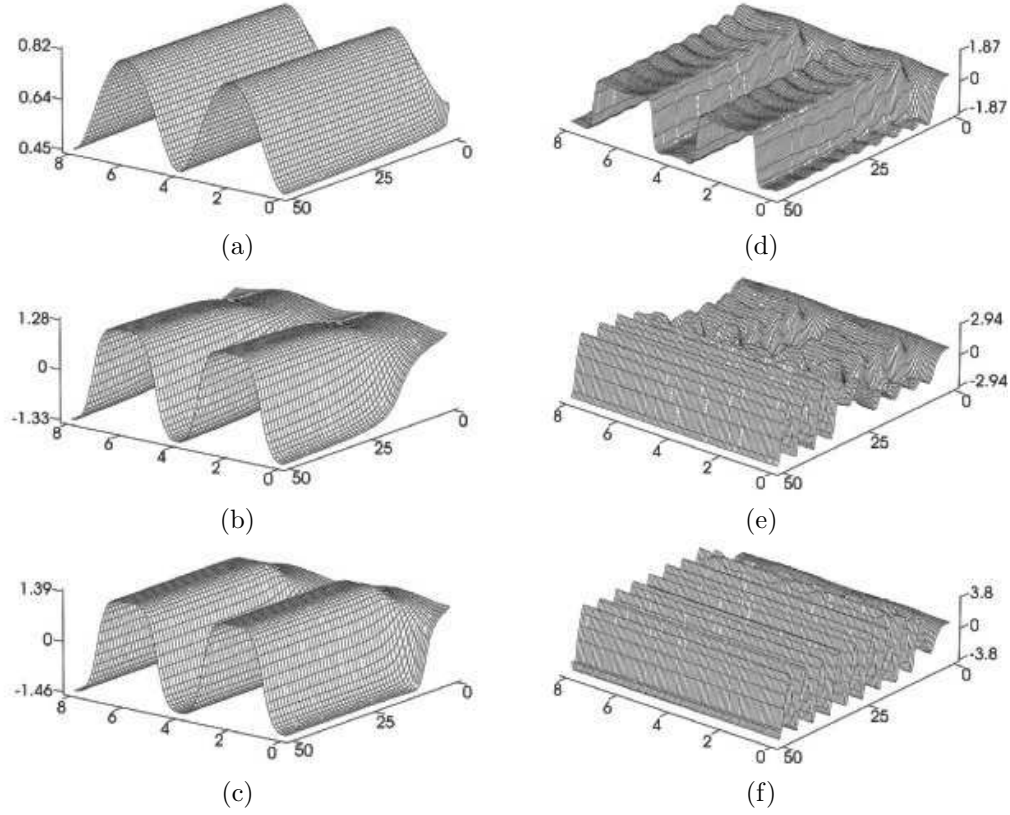


FIG. 4.1. Numerical solution of the fractional reaction-diffusion equations (1.3),(1.4) with nonlinearities (3.1). Dynamics of variable n_1 on the time interval $(0,50)$ for $l_x = 8, \mathcal{A} = -0.1, \beta = 1, \tau_1 = \tau_2 = 1, l^2 = 0.05, L^2 = 1$; (a) $-\alpha=0.1$, (b) $-\alpha=0.5$, (c) $-\alpha=0.99$, (d) $-\alpha=1.5$, (e) $-\alpha=1.6$, (f) $-\alpha=1.8$

in the form of nonhomogeneous dissipative structures are inherent to unstable region $\bar{n}_1 \in (-1, 1)$. Figures 4.1(a)-(c) show the steady state dissipative structure formation and Figures 4.1 (d)-(f) present the spatio-temporal evolution of dissipative structures, which eventually leads to homogeneous oscillations.

On the Figure 4.1(a)-(d), the value α increases from 0.1 to 1.5 and on this whole interval the structures are in steady state. This is due to the case $\alpha < \alpha_0$, the oscillatory perturbations are damping, and we can see that small oscillations are at the transition period n_1 . With increasing α , the steady state structures change to the spatio-temporary behavior (Figure 4.1(e)-(f)).

The emergence of homogeneous oscillations, which destroy pattern formation (Figure 4.1(e),(f)) has deep physical meaning. The matter is that the stationary dissipative structures consist of smooth and sharp regions of variable n_1 , and the smooth shape of n_2 . The linear system analysis shows that the homogeneous distribution of the variables is unstable according to oscillatory perturbations inside the wide interval of \bar{n}_1 , which is much wider then interval $(-1, 1)$. At the same time, smooth distributions at the maximum and minimum values of n_1 are $\pm\sqrt{3}$ correspondingly. In the first approximation, these smooth regions of the dissipative structures resemble homogeneous ones and are located inside the instability regions. As a result, the

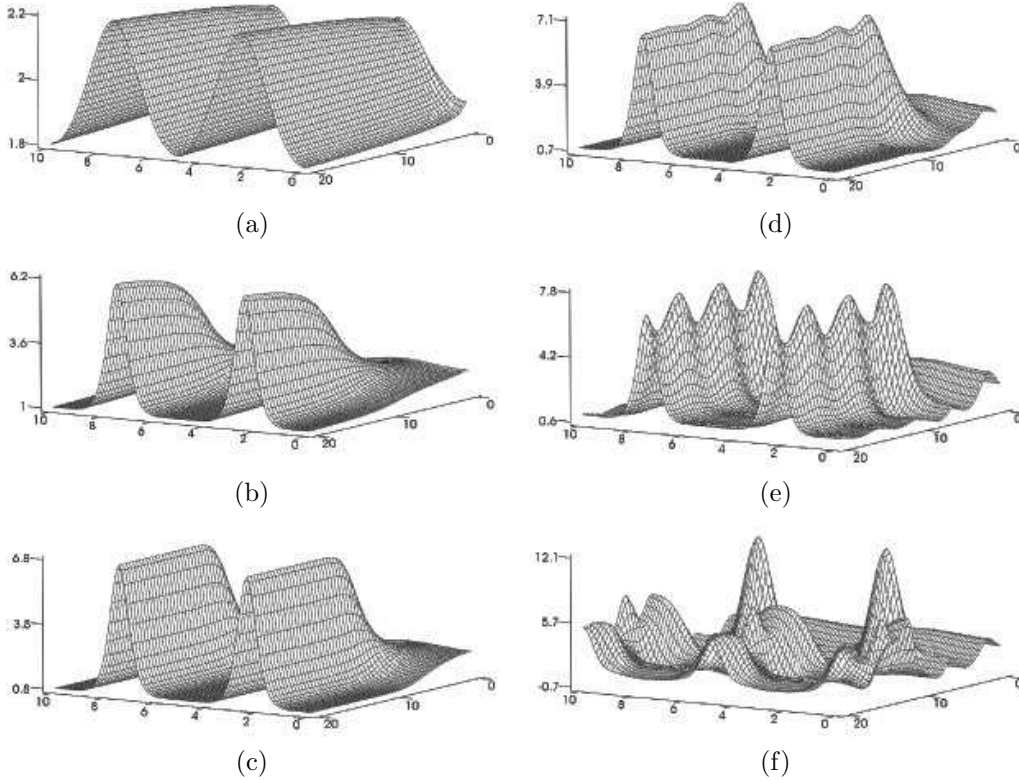


FIG. 4.2. Numerical solution of the fractional reaction-diffusion equations (1.3), (1.4) with nonlinearities (3.2). Dynamics of variable n_1 on the time interval $(0, 20)$ for $l_x = 10$, $\mathcal{A} = 2$, $\beta = 2$, $\tau_1 = \tau_2 = 1$, $l^2 = 0.1$, $L^2 = 10$; (a) - $\alpha = 0.1$, (b) - $\alpha = 0.5$, (c) - $\alpha = 0.99$, (d) - $\alpha = 1.5$, (e) - $\alpha = 1.6$, (f) - $\alpha = 1.8$

unstable fluctuations lead to homogeneous oscillations, and the dissipative structures destroy themselves. We can conclude that oscillatory modes in such type FODEs have a much wider attraction region than the corresponding region of the dissipative structures.

For a wide range of the parameters α , the numerical solutions of the Brusselator problem show similar behavior (Figure 4.2(a)-(d)). The stationary solutions emerge practically in the same way. At small α , we see aperiodic formation of the structures, and approaching α_0 , the damping oscillations of the dissipative structures arise. At $\alpha_0 = 1.7$ certain non-stationary structures arise (Figure 4.2(e)). In this case, the dissipative structures look quite similar to those we obtained for regular system [36, 37]. The increase of α leads to a larger amplitude of pulsation. All these patterns are robust with respect to small initial perturbations. The further increase of α leads to spatially temporary chaos (Figure 4.2(f)).

In the contrast to previous case, such nonhomogeneous behavior is stable and does not lead to homogeneous oscillations. The matter is that in Brusselator model, the dissipative structures are much greater in amplitude and do not have smooth distribution at the top.

It should be noted that the pulsation phenomena of the dissipative structures is

closely related to the oscillation solutions of the ODE (Figures 3.3, 3.4). Moreover, the fractional derivative of the first variable has the most impact on the oscillations emergence. It can be obtained by performing a simulation where the first variable is a fractional derivative and the second one is an integer. It should be emphasized that the distribution of n_2 , within the solution, only shows a small deviation from the stationary value (that is why this variable is not represented in the figures).

5. Conclusion. In this article we developed a linear theory of instability of reaction diffusion system with fractional derivatives. The introduced new parameter – marginal value α_0 plays the role of bifurcation parameter. If the fractional derivative index α is smaller than α_0 , the system of FODEs is stable and has oscillatory damping solutions. At $\alpha > \alpha_0$, the FODEs becomes unstable, and we obtain oscillatory or even more complex - quasi chaotic solutions. In addition, the stable and unstable domains of the system were investigated.

By the computer simulation of the fractional reaction-diffusion systems we provided evidence that pattern formation in the fractional case, at α less than a certain value, is practicably the same as in the regular case scenario $\alpha = 1$. At $\alpha > \alpha_0$, the kinetics of formation becomes oscillatory. At $\alpha = \alpha_0$, the oscillatory mode arises and can lead to homogeneous or nonhomogeneous oscillations. In the last case scenario, depending on the parameters of the medium, we can see a rich variety of spatiotemporal behavior.

REFERENCES

- [1] G. NICOLIS, I. PRIGOGINE. *Self-organization in non-equilibrium systems*. Wiley, New York. 1977.
- [2] M. C. CROSS AND P. S. HOHENBERG. *Pattern formation outside of equilibrium*, Rev. Modern Phys., 65 (1993), pp. 851–1112.
- [3] A. S. MIKHAILOV. *Foundations of Synergetics*, Springer-Verlag, Berlin, 1990.
- [4] B.S. KERNER, V.V. OSIPOV. *Autosolitons* Kluwer, Dordrecht, 1994.
- [5] J. D. DOCKERY AND J. P. KEENER *Diffusive effects on dispersion in excitable media*, SIAM J. Appl. Math., 49 (1989), pp. 539–566.
- [6] A. DOELMAN AND T. J. KAPER. *Semistrong pulse interactions in a class of coupled reaction-diffusion equations* SIAM J. Applied dynamical systems Vol. 2, No. 1, (2003), pp. 53–96.
- [7] A.LUBASHEVSKII, V.V.GAFIYCHUK. *The projection dynamics of highly dissipative system*. Phys. Rev. E. vol.50, No.1, (1994), pp.171–181.
- [8] V.V. GAFIYCHUK, I.A. LUBASHEVSKII. *Variational representation of the projection dynamics and random motion of highly dissipative systems*. J. Math. Phys. v.36. #10, (1995), pp. 5735-5752.
- [9] P.SCHUTZ, M.BODE, V.V.GAFIYCHUK. *Transition from stationary to travelling localized patterns in two-dimensional reaction-diffusion system*. Phys. Rev. E. v.52., N4, (1995), pp. 4465-4473.
- [10] C. B. MURATOV AND V. V. OSIPOV. *Stability of the static spike autosolitons in the Gray-scott model* Siam J. Appl. Math. Vol. 62, no. 5, (2002), pp. 1463–1487.
- [11] M. GOLUBITSKY, D. LUSS AND S.H. STROGATZ. *Pattern Formation in Continuous and Coupled Systems*, IMA Volumes in Mathematics and its Applications 115 , Springer, New York, (1999).
- [12] B.I. HENRY, T.A.M. LANGLANDS AND S.L. WEARNE *Turing pattern formation in fractional activator-inhibitor systems*. Phys. Rev. E., 72, # 026101, (2005).
- [13] B.I. HENRY, S.L. WEARNE. *Fractional reaction-diffusion*. Physica A 276, (2000), pp. 448–455.
- [14] B.I. HENRY AND S.L. WEARNE. *Existence of turing instabilities in a two-species fractional reaction-diffusion system*. Siam J. Appl. Math. Vol. 62, No. 3, (2002), pp. 870–887.
- [15] M. O. VLAD AND J. ROSS. *Systematic derivation of reaction-diffusion equations with distributed delays and relations to fractional reaction-diffusion equations and hyperbolic transport equations: Application to the theory of Neolithic transition*. Phys. Rev. E 66, 061908 (2002).
- [16] K. SEKI, M. WOJCIK, AND M. TACHIYA. *Fractional reaction-diffusion equation*. J. Chem. Phys. 119, 2165, (2003).

- [17] V. GAFIYCHUK, B. DATSKO. *Pattern formation in a fractional reaction-diffusion system*. Physica A: Statistical Mechanics and its Applications. Vol. 365, (2006), pp. 300–306.
- [18] V.V.GAFIYCHUK, B.Y.DATSKO, YU.YU.IZMAJLOVA. Analysis of the dissipative structures in reaction-diffusion systems with fractional derivatives. Math. metody ta phys.-mech. polia. V.49, #4, 2006, pp. 109-116 (in Ukrainian)
- [19] R.K. SAXENA, A.M. MATHAI AND H.J. HAUBOLD. Fractional reaction-diffusion equations. arXiv:math.CA/0604473 v1 21 Apr 2006.
- [20] G.M. ZASLAVSKY AND H. WEITZNER Some Applications of Fractional Equations. E-print nlin.CD/0212024, (2002).
- [21] C. VAREA AND R. A. BARRIO. Travelling Turing patterns with anomalous diffusion. J. Phys.: Condens. Matter 16, (2004), pp. 5081–5090.
- [22] V. E. TARASOV AND G. M. ZASLAVSKY. Nonholonomic constraints with fractional derivatives. J. Phys. A: Math. Gen. 39 (2006), pp. 9797–9815.
- [23] S.G. SAMKO, A. A. KILBAS, AND O. I. MARICHEV, *Fractional Integrals and Derivatives: Theory and Applications*, Gordon and Breach, Newark, N. J., 1993.
- [24] I. PODLUBNY. *Fractional Differential Equations*. Academic Press, 1999.
- [25] Z. M. ODIBAT, N. T. SHAWAGFEH *Generalized Taylor's formula*. *Applied Mathematics and Computation* xxx (2006) xxx-xxx (available online at www.sciencedirect.com)
- [26] R YU, H. ZHANG, *New function of Mittag-Leffler type and its application in the fractional diffusion-wave equation*, Chaos, Solitons and Fractals 30 (2006), pp. 946–955.
- [27] G. ADOMIAN. *Solving Frontier Problems of Physics: The Decomposition Method*, Kluwer Academic Publishers, Dordrecht, 1994.
- [28] J. BIAZAR, E. BABOLIAN, R. ISLAM Solution of the system of ordinary differential equations by Adomian decomposition method, Appl. Math. Comput. 147 (3) (2004), pp. 713–719.
- [29] H. JAFARI, V. DAFTARDAR-GEJJI. *Solving a system of nonlinear fractional differential equations using Adomian decomposition*. Journal of Computational and Applied Mathematics 196 (2006), pp. 644 - 651
- [30] V. DAFTARDAR-GEJJI, A. BABAKHANI. Analysis of a system of fractional differential equations, J. Math. Anal. Appl. 293 (2004), pp. 511–522.
- [31] G.M. ZASLAVSKY, A.A. STANISLAVSKY, M. EDELMAN Chaotic and Pseudochaotic Attractors of Perturbed Fractional Oscillator, arXiv:nlin.CD/0508018.
- [32] D. MATIGNON, *Stability results for fractional differential equations with applications to control processing*, Computational Eng. in Sys. Appl., Vol. 2, Lille, France 963, 1996.
- [33] A.M.A. EL-SAYED. *Fractional differential-difference equations*, J. Fract. Calc. 10 (1996), pp. 101–106.
- [34] H.WEITZNER, G.M.ZASLAVSKY. *Some applications of fractional equations*. Communications in Nonlinear Science and Numerical Simulation 8 (2003), pp. 273–281.
- [35] K.D.OLDHAM AND J.SPANIER *The Fractional Calculus: Theory and Applications of Differentiation and Integration to Arbitrary Order, Vol.111 of Mathematics in Science and Engineering* Academic Press, New York, 1974.
- [36] V.V.GAFIYCHUK, B.S.KERNER, V.V.OSIPOV, T.M.SCHERBATCHENKO. Formation of pulsating thermal-diffusion autosolitons and turbulence in a nonequilibrium electron-hole plasma. Sov. Phys. Sem. (USA). v.25, #11, (1991) (Translation of Fiz.Tekh. Poluprovodn (USSR). v.25, No.11, (1991), pp. 1696–1702).
- [37] V.V.GAFIYCHUK, A.V.DEMCHUK. Analysis of the dissipative structures in Gierer-Meinhardt model. Matematicheskie metody i physico-mechanicheskie polia. V.40, #2, 1997, pp.48-53 (in Ukrainian, English translation in Journal of Mathematical Sciences, v.88, #4, 1998).